Device Characteristics of Organic Light-Emitting Diodes Comprising Terfluorene Modified with Triphenyltriazine

Andrew C.-A. Chen,[†] Jason U. Wallace,[†] Kevin P. Klubek,[†,‡] Marcel B. Madaras,[‡] Ching W. Tang,*[,†] and Shaw H. Chen*[,†,§]

Department of Chemical Engineering and Laboratory for Laser Energetics, 240 East River Road, University of Rochester, Rochester, New York 14623-1212, and Kodak Research Laboratories, Eastman Kodak Company, 1999 Lake Avenue, Rochester, New York 14650-2116

Received March 14, 2007. Revised Manuscript Received June 5, 2007

The characteristics of a series of organic blue light-emitting diodes comprising terfluorene were investigated. The composition of the emitter layer was either a neat terfluorene compound, **F(MB)3**, **F(MB)3** doped with **TRZ**, triphenyltriazine, as an electron acceptor, or hybrid compounds, **TRZ-3F-(MB)3** and **TRZ-1F(MB)3**, viz. **TRZ** functionalized with **F(MB)3**. The emitter layer was deposited by spin-casting from a solution on top of a **PEDOT:PSS** hole-injecting layer. These acceptor-containing emitters were responsible for a decreasing electroluminescence efficiency with an increasing **TRZ** content. The loss of efficiency can be attributed to an enhanced electron transport through the emitter layer and a consequent shift of the electron−hole recombination zone toward the exciton-quenching **PEDOT:PSS** interface. Compared to **TRZ** as the electron-accepting dopant in **F(MB)3**, **TPBI** caused a more substantial decrease in emission efficiency and a more pronounced rise in drive voltage presumably because of the protonation of **TPBI** by **PEDOT:PSS** to a much greater extent.

Introduction

Organic electroluminescence has been intensely investigated over the past two decades because of its promise for a new generation of flat-panel displays beyond liquid crystal displays and for efficient solid-state lighting.[1] Both fluorescent and phosphorescent materials have been widely explored, including molecular materials that can be vacuum deposited[2,3] and π-conjugated polymers[4] that can be solution processed. To fully exploit the potential of organic light-emitting diodes, OLEDs, continuing efforts have been devoted to significantly improving device efficiency and lifetime.[5,6] Relevant issues include chemical purity, morphological stability, balanced fluxes of electrons and holes through the emitter layer, and degradation of materials and contacts. Blue-emitting OLEDs have remained the most challenging of the three primary emissive colors in terms of device stability.

Because of the cost advantage, organic materials that can be solution processed into noncrystalline films are of particular interest. Among these solution processable materials, fluorene-based polymers and oligomers hold enormous potential because of their high efficiency in blue fluorescence.[7] In particular, oligofluorenes are highly desirable in view of their well-defined and uniform molecular structures as well as superior chemical purity acquired through recrystallization and/or column chromatography,[8] all associated with the monodispersity and low molecular weights of oligomers relative to polymers. These intrinsic merits are crucial to gaining fundamental insight into structure−property relationships and to improving OLED device performance. As a potentially viable approach to improving OLED device efficiency and lifetime, we have further introduced a class of blue-emitting hybrid materials with tunable charge injection and transport properties.[9] Specifically, monodisperse oligofluorenes are attached via an alkyl spacer to an electron- or hole-conducting core not only to retain independent functions of the two structural elements without electronic interference but also to achieve an elevated

* To whom correspondence should be addressed. E-mail: chtang@che.rochester.edu (C.W.T.); shch@lle.rochester.edu (S.H.C.).
[†] Department of Chemical Engineering, University of Rochester.
[‡] Eastman Kodak Company.
[§] Laboratory for Laser Energetics, University of Rochester.

(1) (a) *Organic Electroluminescence*; Kafafi, Z. H., Ed.; Optical Engineering Vol. 94; Taylor and Francis: Boca Raton, FL, 2005. (b) *Organic Light-Emitting Diodes: Principles, Characteristics, and Processes*; Kalinowski, J., Ed.; Optical Engineering Vol. 91; Marcel Dekker: New York, 2005. (c) *Organic Light-Emitting Devices: A Survey*; Shinar, J. Ed.; Springer-Verlag: New York, 2004. (d) D'Andrade, B. W.; Forrest, S. R. *Adv. Mater.* **2004**, *16*, 1585.
(2) Tang, C. W.; VanSlyke, S. A. *Appl. Phys. Lett.* **1987**, *51*, 913.
(3) Baldo, M. A.; O' Brien, D. F.; You, Y.; Shoustikov, A.; Sibley, S.; Thompson, M. E.; Forrest, S. R. *Nature* **1998**, *395*, 151.
(4) Burroughes, J. H.; Bradley, D. D. C.; Brown, A. R.; Marks, R. N.; Mackay, K.; Friend, R. H.; Burns, P. L.; Holmes, A. B. *Nature* **1990**, *347*, 539.
(5) Patel, N. K.; Ciná, S.; Burroughes, J. H. *IEEE J. Sel. Top. Quantum Electron* **2002**, *8*, 346 and references therein.
(6) Aziz, H.; Popovic, Z. D. *Chem. Mater.* **2004**, *16*, 4522.
(7) (a) Bernius, M. T.; Inbasekaran, M.; O' Brien, J.; Wu, W. *Adv. Mater* **2000**, *12*, 1737. (b) Neher, D. *Macromol. Rapid Commun.* **2001**, *22*, 1365. (c) Scherf, U.; List, E. J. W. *Adv. Mater.* **2002**, *14*, 477.
(8) (a) Geng, Y.; Trajkovska, A.; Katsis, D.; Ou, J. J.; Culligan, S. W.; Chen, S. H. *J. Am. Chem. Soc.* **2002**, *124*, 8337. (b) Geng, Y.; Culligan, S. W.; Trajkovska, A.; Wallace, J. U.; Chen, S. H. *Chem. Mater.* **2003**, *15*, 542. (c) Geng, Y.; Chen, A. C. A.; Ou, J. J.; Chen, S. H.; Klubek, K.; Vaeth, K. M.; Tang, C. W. *Chem. Mater.* **2003**, *15*, 4352. d) Klaerner, G.; Miller, R. D. *Macromolecules* **1998**, *31*, 2007. (e) Jo, J.; Chi, C.; Höger, S.; Wegner, G.; Yoon, D. Y. *Chem.—Eur. J.* **2004**, *10*, 2681.
(9) (a) Chen, A. C. A.; Wallace, J. U.; Wei, S. K.-H.; Zeng, L.; Chen, S. H. *Chem. Mater.* **2006**, *18*, 204. (b) Chen, A. C. A.; Madaras, M. B.; Klubek, K. P.; Wallace, J. U.; Wei, S. K.-H.; Zeng, L.; Chen, S. H. *Chem. Mater.* **2006**, *18*, 6083.

10.1021/cm0707105 CCC: $37.00
Published on Web 07/17/2007

Scheme 1. Synthesis of TRZ-1F(MB)3.

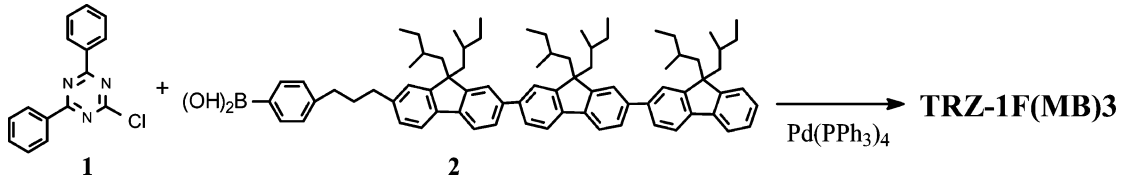

glass-transition temperature with improved stability against crystallization over the stand-alone oligofluorenes reported previously.[8]

This study was undertaken to understand the effect of the emitter layer's chemical composition on the OLED efficiency through the modulation of the layer's transport properties. Oligofluorenes, specifically terfluorenes, were used as the emitter, providing the emitting chromophore as well as the bipolar transport component. The carrier transport properties in the emitter layer were modified by either using an electron-acceptor moiety chemically linked to the terfluorene structure or by forming a homogeneous film of the terfluorene doped with an electron-acceptor. The influence of the interfaces bounding the emitter layer on the OLED efficiency was also elucidated.

Experimental Section

Material Synthesis and Characterization. The synthesis and properties of **F(MB)3**, **TRZ-3F(MB)3**, and intermediate **2** have been reported elsewhere.[9] Intermediate **1** was prepared following previously reported procedures.[10] **TRZ-1F(MB)3**, 2-[*p*-3-(ter(9,9-bis(2-methyl-butyl)fluoren-7-yl)propyl-phenyl]-4,6-diphenyl-triazine, was synthesized following Scheme 1; synthesis and purification procedures are described in the Supporting Information. The chemical purity and molecular structures were elucidated with elemental analysis, ^{1}H NMR spectroscopy, and MALD/I−TOF mass spectrometry. **TRZ-1F(MB)3**, ^{1}H NMR (400 MHz, $CDCl_3$): δ 8.80−8.83 (d, 4H), 8.73−8.75 (d, 2H), 7.76−7.84 (m, 5H), 7.59−7.71 (m, 15H), 7.31−7.44 (m, 5H), 7.21−7.27 (m, 2H), 2.80−2.84 (t, 4H), 2.11−2.25 (m, 8H), 1.93−1.98 (m, 6H), 0.60−1.01 (m, 36H), 0.30−0.45 (m, 18H). Molecular weight calcd. for $C_{237}H_{285}N_3$: 1264.9. MALD/I−TOF MS (DCTB) *m*/*z* ($[M]^+$): 1264.0. Anal. Calcd. for $C_{237}H_{285}N_3$: C, 88.31; H, 8.37; N, 3.32. Found: C, 88.11; H, 8.34; N, 3.27. The chemical purities of **TRZ-3F(MB)3**, **TRZ-1F(MB)3**, and **F(MB)3** were further validated with <20 ppm contents of Cl, Br, and I by neutron activation analysis.

Molecular Structures, Morphology, and Phase-Transition Temperatures. ^{1}H NMR spectra were acquired in $CDCl_3$ with an Avance 400 spectrometer (400 MHz). Elemental analysis was carried out by Quantitative Technologies, Inc. Molecular weights were measured with a TofSpec2E MALD/I−TOF mass spectrometer (Micromass, Inc., U.K.). Thermal-transition temperatures were determined by differential scanning calorimetry (Perkin-Elmer DSC-7) with a continuous N_2 purge at 20 mL/min. Samples were preheated to 260 °C followed by cooling at −20 °C/min to −30 °C before taking the reported second heating scans at 20 °C/min.

Preparation and Characterization of Neat Films. Optically flat fused silica substrates (25.4 mm diameter × 3 mm thickness, transparent to 200 nm, Esco Products) were cleaned prior to use. Glassy isotropic films were prepared by spin-coating from 0.5 wt % solutions in chloroform at 4000 rpm followed by drying in vacuo overnight. Absorption spectra were gathered with an HP 8453E UV−vis−NIR diode array spectrophotometer. Fluorescence spectra were collected with a spectrofluorimeter (Quanta Master C-60SE, Photon Technology International) at an excitation wavelength of 360 nm. Optical constants and thickness of thin films were determined with reflection mode spectroscopic ellipsometry (V-VASE, J. A. Woollam Co.). The film thicknesses of all four deep-blue emitters prepared under the same conditions turned out to be 50 ± 1 nm. Refractive indices were used to evaluate the photoluminescence quantum yield following a procedure reported previously.[8a]

Electrochemical Characterization. An electrochemical analyzer (model CHI660, CH Instruments, Inc., Austin, TX) was employed to perform the cyclic voltammetric measurements. A glassy carbon electrode was adopted as the working electrode to take advantage of its wider electrical potential window relative to that of the Pt electrode in this system. This electrode ($A = 0.071$ cm^2) was cleaned and activated by electrochemical treatment prior to use. A platinum wire served as the auxiliary electrode. A saturated calomel electrode was used as a quasi-reference electrode to complete a standard 3-electrode electrochemical cell. The supporting electrolyte, tetrabutylammonium tetrafluoroborate (>98%, Fluka), was purified by dissolution in a minimum amount of ethanol for treatment with activated charcoal followed by filtration through Celite powder and addition of water (twice the volume of the ethanol) for recrystallization at 0 °C. Recrystallization was repeated until the oxidation and reduction scans attributable solely to the electrolyte were observed. Energy levels were estimated relative to ferrocene's HOMO level of 4.8 eV.[11]

OLED Device Fabrication and Characterization. Glass substrates (Polytronix) coated with patterned indium tin oxide (ITO) were thoroughly cleaned and treated with oxygen plasma prior to spin-casting a 400 Å thick **PEDOT:PSS** layer. The emitter layers were then prepared on the **PEDOT:PSS** layer by spin-coating from 1.8 wt % toluene solutions at 4000 rpm resulting, in a thickness of 530 ± 20 Å for thin films. An electron-transport layer was prepared via thermal evaporation of **TPBI** at a base pressure of 5×10^{-6} Torr or lower at a deposition rate of 4 Å/s. Through co-dissolution in toluene, **TRZ** and **TPBI** were mixed with **F(MB)3** at a concentration of up to 10 wt %, and **DSB** was coevaporated with **TPBI** at a concentration of 1 wt % for the luminescence sensing experiment. The magnesium:silver cathode (Mg:Ag) was deposited by coevaporation at 10 and 1 Å/s, respectively. All devices were not encapsulated for characterization with a source-measure unit (Keithley 2400) and a spectroradiometer (PhotoResearch PR650).

Results and Discussion

The molecular structures and labels for the materials used in this study are shown in Chart 1. Terfluorene **F(MB)3** was the base material and **TRZ-3F(MB)3** was a hybrid compound consisting of 3:1 **F(MB)3**:**TRZ** mole ratio. Both were reported previously.[9] **TRZ-1F(MB)3** was a new hybrid compound consisting of 1:1 ratio of **F(MB)3** to **TRZ**. **TRZ**

(10) Henneberger, H.; Wagner, M. U.S. Patent 5 438 138, 1995.

(11) Fink, R.; Heischkel, Y.; Thelakkat, M.; Schmidt, H. W.; Jonda, C.; Hüppauff, M. *Chem. Mater.* **1998**, *10*, 3620.

Chart 1. Molecular Structures of Organic Compounds Used in the Emitter Layer and the Electron-Transport Layer (glass-transition temperature, PL quantum efficiency, and HOMO/LUMO energy levels are included in the inset).

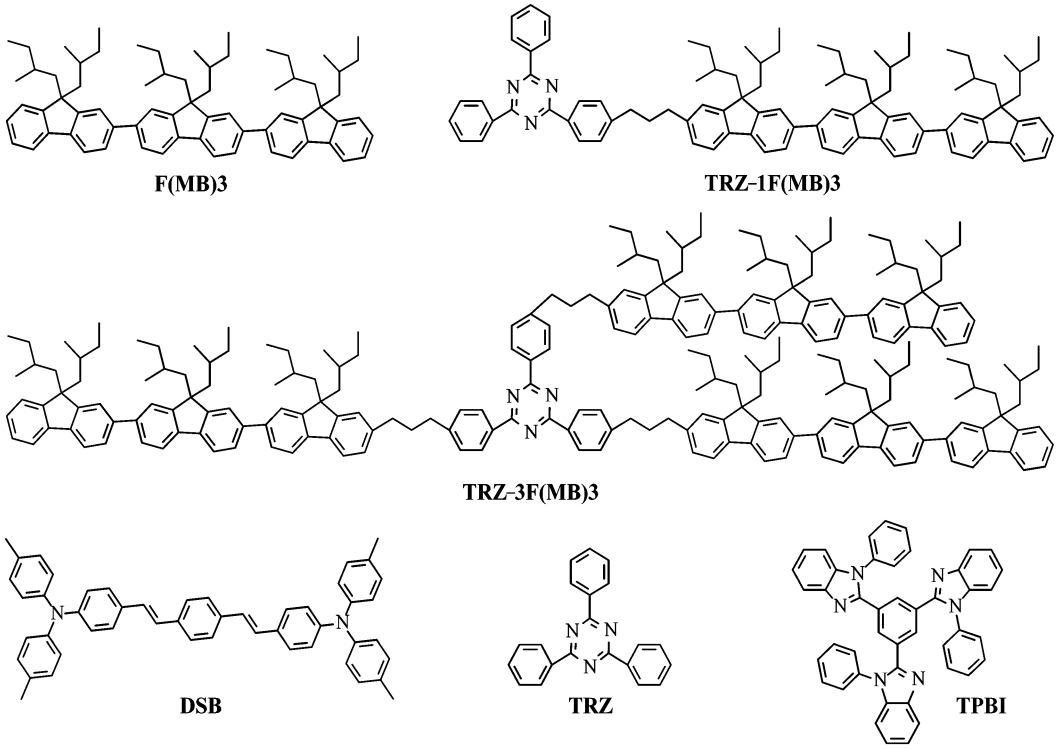

Compound	T_g °C	Φ_{PL} [a] %	HOMO eV	LUMO eV
F(MB)3	56	68	−5.64	−2.07
TRZ-3F(MB)3	87	51	−5.63	−2.57
TRZ-1F(MB)3	75	59	−5.60	−2.62

[a] Φ_{PL} accompanied by an experimental uncertainty of ±4%.

is a known electron acceptor,[12] and its incorporation in the hybrid compounds was intended to produce a material with an appropriate LUMO level and enhanced electron-transport properties. The chemical purities of **F(MB)3** and the hybrid compounds were validated with elemental analysis, ^{1}H NMR spectroscopy, MALD/I−TOF mass spectrometry, and neutron activation for the analysis of halogen impurities. **TRZ** and **TPBI** were purified by vapor sublimation before use.

The glass-transition temperature T_g, photoluminescence quantum yield, Φ_{PL}, and the HOMO and LUMO energy levels are tabulated as part of Chart 1. Note that the LUMO levels of **TRZ-3F(MB)3** (−2.57 eV) and **TRZ-1F(MB)3** (−2.62 eV) are similar and significantly lower than that of **F(MB)3** (−2.07 eV), consistent with the expectation that the LUMO levels for the hybrid molecules are associated with the **TRZ** core.[11] The presence of the low-lying **TRZ**'s LUMO level is expected to facilitate electron injection. The HOMO levels are practically identical for all three compounds, indicating that they reside in the **F(MB)3** pendants.

The device structure and energy levels for the series of OLED devices are shown in Figure 1. Sandwiched between the ITO/**PEDOT:PSS** anode and Mg:Ag cathode are (1) the terfluorene-emitting layer (530 Å) prepared by spin-casting on top of the **PEDOT:PSS** layer (400 Å), and (2) the **TPBI** electron-transport layer (300 Å) deposited on top of the emitter layer by vapor deposition. The work function values for ITO, **PEDOT:PSS**, and Mg:Ag were taken from literature;[13] the HOMO and LUMO levels of the organic compounds were derived from the redox potentials obtained from cyclic voltammetry.[11]

Table 1 summarizes the electroluminescence (EL) data obtained under a constant current density of 20 mA/cm^2. It can be seen that the color coordinates are nearly the same regardless of the variation in the emitter-layer composition. The blue EL emission has a spectral characteristic essentially identical to the PL of a neat **F(MB)3** film, indicating that the **F(MB)3** component is solely responsible for the EL emission, independent of the chemical composition of the

(12) Kulkarni, A. P.; Tonzola, C. J.; Babel, A.; Jenekhe, S. A. *Chem. Mater.* **2004**, *16*, 4556.

(13) (a) Shi, J.; Tang, C. W. *Appl. Phys. Lett.* **2002**, *80*, 3201. (b) Yan, H.; Scott, B. J.; Huang, Q.; Marks, T. J. *Adv. Mater.* **2004**, *16*, 1948.

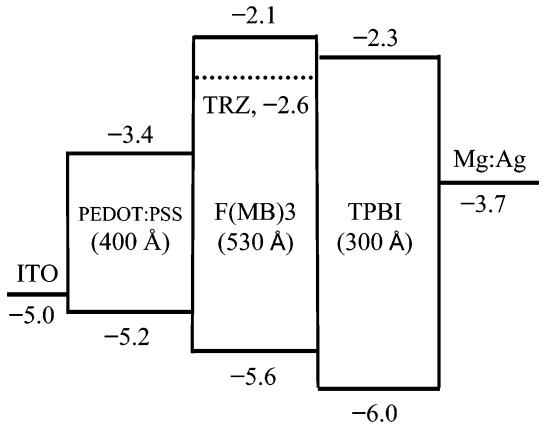

Figure 1. OLED device structure and energy level diagram expressed in electron volts.

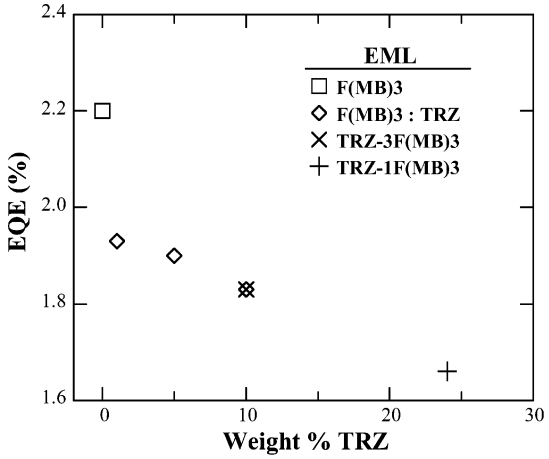

Figure 2. Plot of EQE vs **TRZ** concentration for cells A−F.

emitter layer, i.e., with or without **TRZ** or **TPBI** as electron acceptor. It should be noted that the use of **TPBI** as the electron-transport layer is essential to obtaining efficient blue EL emission from **F(MB)3**, as **TPBI** effectively blocks both hole and exciton transfer from the **F(MB)3** emitter layer. Substituting **TPBI** with tris-(8-hydroxyquinoline)aluminum, **Alq$_3$**, which has a smaller energy gap and a deeper LUMO compared to **F(MB)3**, yielded only green emission from **Alq$_3$**. Similar results have been reported for other oligofluorene emitters.[14]

Comparing OLED efficiencies and drive voltages in Table 1, it is noted that the external quantum efficiency, EQE, for cell A with a neat **F(MB)3** film as the emitting layer is the best in the series. It has a drive voltage of 6.2 V and an EQE of 2.20%. Replacing **F(MB)3** with the hybrid compounds **TRZ-3F(MB)3** (cell B) or **TRZ-1F(MB)3** (cell C) appears to depress the EQE and raise the drive voltage, albeit only modestly. The lower EQE may be related to a lower photoluminescence yield, Φ_{PL}, found in the hybrid compounds (see Figure 1), but the Φ_{PL} and EQE trends between the hybrid compounds are inconsistent with each other. A more plausible explanation is that the efficiency loss is caused by a shift of the electron−hole recombination zone toward

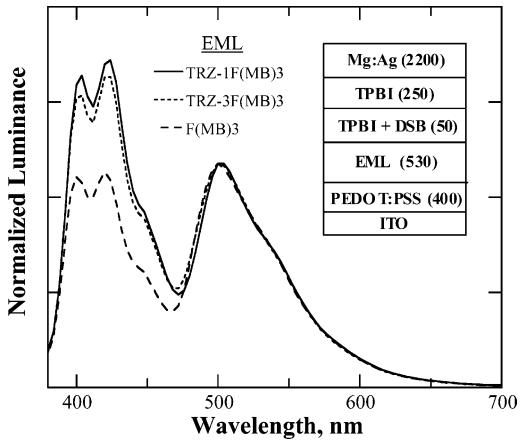

Figure 3. Normalized electroluminescence spectra and device structure comprising **TRZ-1F(MB)3**, **TRZ-3F(MB)3**, and **F(MB)3** with a probing layer of **DSB**-doped **TPBI** at a current density of 20 mA/cm^2; the numbers in parentheses indicate layer thickness in angstroms.

the **PEDOT:PSS** interface, which is known to quench excitons efficiently.[15] The observed trend in EQE: **F(MB)3** > **TRZ-3F(MB)3** > **TRZ-1F(MB)3** is consistent with such a shift being caused by an enhanced electron transport in the emitter layers with an increasing electron acceptor content. The proposed shift in the electron−hole recombination zone is supported by luminescence sensing as reported in Figure 3 below.

TRZ-3F(MB)3 and **TRZ-1F(MB)3** were originally intended for use in an emitter layer, where the transport and luminescence properties can be tailored with a single molecular entity. As shown in cells A−C, the modulation of the electron transport property is consistent with the molecular design, but it turns out that the effect can also be realized simply by using a physical mixture of two components. cells D−F were constructed where the emitter layer was a homogeneously mixed film of **F(MB)3** containing 1, 5, and 10 wt % **TRZ,** respectively. For comparison, the equivalent concentrations of **TRZ** in **TRZ-3F(MB)3** and **TRZ-1F(MB)3** are 10 and 24 wt %, respectively, with **TRZ-1F(MB)3** reaching higher doping levels than possible for the physically doped films. It can be seen in Table 1 that although the difference in EQE between these cells is small, the EQE decreases with increasing wt % **TRZ** in the film, similar to what has been observed in the hybrid compounds. A plot of EQE vs wt % **TRZ** for cells A−F (Figure 2) shows a steady decrease in the EQE with increasing **TRZ** concentration, suggesting that the effect of **TRZ** on EQE is related to its concentration regardless of the means by which it is incorporated in the emitter layer. The higher drive voltage (7.34 and 7.46V) found in cells D and E is attributed to a low concentration of **TRZ** in these films, which can give rise to electron transport limited by trap-to-trap hopping.[16] This voltage rise could also be explained by morphological or packing differences in the physically doped films.

(14) Wu, C.-C.; Lin, Y.-T.; Wong, K.-T.; Chen, R.-T.; Chien, Y.-Y. *Adv. Mater.* **2004**, *16*, 61.

(15) (a) Kim, J.-S.; Ho, P. K. H.; Murphy, C. E.; Seeley, A. J. A. B.; Grizzi, I.; Burroughes, J. H.; Friend, R. H. *Chem. Phys. Lett.* **2004**, *386*, 2. (b) Kim, J.-S.; Friend, R. H.; Grizzi, I.; Burroughes, J. H. *Appl. Phys. Lett.* **2005**, *87*, 023506.

(16) Fishchuk, I. I.; Kadashchuk, A. K.; Vakhnin, A.; Korosko, Y.; Bässler, H.; Souharce, B.; Scherf, U. *Phys. Rev. B* **2006**, *73*, 115210.

Table 1. Characteristics of OLED Cells at a Current Density of 20 mA/cm^2

Cell	Emitting layer (EML) 530 Å	Voltage[a] (V)	EQE[b] (*p*/*e*, %)	CIE (*x*,*y*)
A	**F(MB)3**	6.21	2.20	(0.163, 0.060)
B	**TRZ-3F(MB)3**	6.56	1.83	(0.161, 0.040)
C	**TRZ-1F(MB)3**	6.64	1.66	(0.160, 0.036)
D	**F(MB)3** + 1 wt % **TRZ**	7.34	1.93	(0.163, 0.069)
E	**F(MB)3** + 5 wt % **TRZ**	7.46	1.90	(0.164, 0.080)
F	**F(MB)3** + 10 wt % **TRZ**	7.01	1.83	(0.164, 0.075)
G	**F(MB)3** + 1 wt % **TPBI**	8.75	0.61	(0.167, 0.073)
H	**F(MB)3** + 5 wt % **TPBI**	10.50	0.48	(0.165, 0.067)

[a] Drive voltage with an uncertainty of ±0.2 V. [b] EQE with an uncertainty of ±0.04%.

Although a further increase in **TRZ** concentration in **F(MB3)**:**TRZ** mixed films could lower the drive voltage, it was found that a **TRZ** content of 25 wt % resulted in failed OLED devices because of phase separation in the emitter layer, as evidenced by the presence of microcrystalline **TRZ**.

To further explore the mixed films, we replaced **TRZ** by **TPBI** in the emitter layer in cells G and H. Because **TPBI** was also used for the electron-transport layer in these cells, one would expect near alignment of LUMO levels between the emitter layer and the electron-transport layer, and therefore efficient electron injection into the emitter layer. Because **TPBI** has a higher LUMO level than **TRZ** and a substantially different molecular structure, electron transport in the mixed films and its effect on OLED performance could be quite different. A lower electron mobility in **TPBI**[17] would favor a recombination zone closer to the electron-transport layer interface and therefore a higher EQE. To the contrary, the EQE values of the **TPBI**-doped cells (G and H) were found to be much lower than the **TRZ** doped cells (D and E), 0.61 and 0.48% compared to 1.93 and 1.90%, respectively. In addition, drive voltages were much higher. The unexpectedly poor device performance can be understood by examining the **PEDOT:PSS** interface using **F(MB)3** doped with **TPBI**. Note the much higher pK_a value of 4.91 for **TPBI** than 1.18 of **TRZ**,[18] indicating that **TPBI** is much more prone to protonation. It is possible that an acid−base reaction occurred between **PEDOT:PSS** and the adjacent **F(MB)3:TPBI** layer, resulting in a build up of positive space charges at the **PEDOT:PSS** interface due to the protonation of **TPBI**. Hole injection into the emitter layer would therefore be reduced or blocked, causing a large increase in drive voltage as well as a large decrease in efficiency as the recombination zone was shifted closer to the **PEDOT:PSS** interface.

Further evidence for a recombination zone shift toward the **PEDOT:PSS** interface, where the hybrid compounds were used as the emitter layer, can be found in the analysis of the EL emission spectra obtained from OLED devices with a layer structure shown as the inset in Figure 3. A thin green-emitting layer (**TPBI** + **DSB**) between the blue-emitting **F(MB)3** emitter layer and the **TPBI** electron-transport layer is used as a luminescence probe to sense the relative recombination probability at the electron-transport interface. The ratio of the intensity of green vs blue emission is taken as a measure of the EL emission from the **TPBI** interface relative to that from the **PEDOT:PSS** interface. It can be seen that the green to blue EL intensity ratio increases in the order **F(MB)3** > **TRZ-3F(MB)3** > **TRZ-1F(MB)3**, i.e., with increasing **TRZ** content in the emitter layer. This trend parallels that in efficiency loss and supports the mechanism that the recombination zone is shifted toward the **PEDOT:PSS** interface as a result of an increasing **TRZ** content in the emitter layer.

Conclusions

This study unravels how the emitter layer's chemical composition can affect OLED device performance through the variation in molecular orbital energy levels, the electron−hole recombination zone relative to interfaces, and the nature of chemical interaction at interfaces. Using **F(MB)3** doped with **TRZ** at various concentrations as well as hybrid compounds **TRZ-3F(MB)3** and **TRZ-1F(MB)3** as the emitter layer, we found that the EL efficiency decreased with an increasing electron-accepting **TRZ** content. Moreover, within the miscibility limit, the effects on EL efficiency is independent of how the acceptor component was introduced in the emitter layer: chemical modification or physical doping. The loss of efficiency is attributed to an enhanced electron transport in the emitter layer, causing a shift of the recombination zone toward the hole-injecting **PEDOT:PSS** interface where exciton quenching is prevalent. It is also noted that through chemical modification, a high **TRZ** content, e.g., 24 wt % in **TRZ-1F(MB)3**, can be achieved without encountering phase separation. In contrast, physical doping of **TRZ** in **F(MB)3** at 25 wt % resulted in OLED device failure because of phase separation. The shift in electron−hole recombination was corroborated with luminescence sensing, which revealed an increasing blue emission relative to the probe's green emission with a deeper electron transport into the emitter layer as a result of an increasing **TRZ** content: **F(MB)3** < **TRZ-3F(MB)3** < **TRZ-1F(MB)-3**. As an alternative electron-acceptor, **TPBI** was doped in **F(MB)3** instead of **TRZ** up to 5 wt %, resulting in a more pronounced decrease in EL efficiency presumably because of the degradation of the hole-injection interface through the protonation of **TPBI** by **PEDOT:PSS**. The suspected degradation of the **PEDOT:PSS** interface was responsible for a significant drive voltage increase accompanying the efficiency drop with **TPBI** present in the emitter layer.

Acknowledgment. The authors thank Myron Culver for his assistance in OLED device fabrication, Dr. Andrew Hoteling and Dr. Craig Swanson for MALD/I−TOF MS and neutron

(17) (a) Hung, W.-Y.; Ke, T.-H.; Lin, Y. T.; Wu, C.-C.; Hung, T.-H.; Chao, T. C.; Wong, K. T.; Wu, C.-I. *Appl. Phys. Lett.* **2006**, *88*, 064102. (b) Ishi-I, T.; Yaguma, K.; Thiemann, T.; Yashima, M.; Ueno, K.; Mataka, S. *Chem. Lett.* **2004**, *33*, 1244.

(18) (a) Walba, H.; Isensee, R. W. *J. Org. Chem.* **1961**, *26*, 2789. (b) Charton, M. *J. Org. Chem.* **1965**, *30*, 3346.

activation analysis, all of Eastman Kodak Company. Financial support was provided by the Eastman Kodak Company and the New York State Center for Electronic Imaging Systems. Additional funding was provided by the Department of Energy Office of Inertial Confinement Fusion under Cooperative Agreement DE-FC03-92SF19460 with the Laboratory for Laser Energetics and the New York State Energy Research and Development Authority. The support of the DOE does not constitute an endorsement by the DOE of the views expressed in this article. Finally, J.W. acknowledges a Horton Graduate Fellowship awarded by the Laboratory for Laser Energetics.

Supporting Information Available: Procedures for the synthesis and purification of **TRZ-1F(MB)3**, its MALD/I−TOF and ^{1}H NMR spectra (PDF), and the analytical data. This material is available free of charge via the Internet at http://pubs.acs.org.

CM0707105